OPEN

Reduced cleavage of von willebrand factor by ADAMTS13 is associated with microangiopathic acute kidney injury following trauma

William E. Plautz[a], Shannon H. Haldeman[b], Mitchell R. Dyer[b], Jason L. Sperry[b], Francis X. Guyette[c], Patricia A. Loughran[b], Jurgis Alvikas[b], Adnan Hassoune[b], Lara Hoteit[b], Nijmeh Alsaadi[b], Brian S. Zuckerbraun[b], Marian A. Rollins-Raval[d,e], Jay S. Raval[d,e], Roberto I. Mota[b,*] and Matthew D. Neal[b,*], A TACTIC Publication

Acute kidney injury (AKI) is common after trauma, but contributory factors are incompletely understood. Increases in plasma von Willebrand Factor (vWF) with concurrent decreases in ADAMTS13 are associated with renal microvascular thrombosis in other disease states, but similar findings have not been shown in trauma. We hypothesized that molecular changes in circulating vWF and ADAMTS13 promote AKI following traumatic injury. VWF antigen, vWF multimer composition and ADAMTS13 levels were compared in plasma samples from 16 trauma patients with and without trauma-induced AKI, obtained from the Prehospital Air Medical Plasma (PAMPer) biorepository. Renal histopathology and function, vWF and ADAMTS13 levels were assessed in parallel in a murine model of polytrauma and haemorrhage. VWF antigen was higher in trauma patients when compared with healthy controls [314% (253–349) vs. 100% (87–117)] [median (IQR)], while ADAMTS13 activity was lower [36.0% (30.1–44.7) vs. 100.0% (83.1–121.0)]. Patients who developed AKI showed significantly higher levels of high molecular weight multimeric vWF at 72-h when compared with non-AKI counterparts [32.9% (30.4–35.3) vs. 27.8% (24.6–30.8)]. Murine plasma cystatin C and vWF were elevated postpolytrauma model in mice, with associated decreases in ADAMTS13, and immunohistologic analysis demonstrated renal injury with small vessel plugs positive for fibrinogen and vWF. Following traumatic injury, the vWF-ADAMTS13 axis shifted towards a prothrombotic state in both trauma patients and a murine model. We further demonstrated that vWF-containing, microangiopathic deposits were concurrently produced as the prothrombotic changes were sustained during the days following trauma, potentially contributing to AKI development. *Blood Coagul Fibrinolysis* 33:14–24 Copyright © 2021 The Author(s). Published by Wolters Kluwer Health, Inc.

Blood Coagulation and Fibrinolysis 2022, **33**:14–24

Keywords: acute kidney injury, ADAMTS13 protein, thrombophilia, von Willebrand factor, wounds and injuries

[a]University of Pittsburgh School of Medicine, [b]Pittsburgh Trauma Research Center and the Department of Surgery, [c]Department of Emergency Medicine, University of Pittsburgh, Pittsburgh, Pennsylvania, [d]Department of Pathology, University of North Carolina –Chapel Hill, Chapel Hill, North Carolina and [e]Department of Pathology, University of New Mexico, Albuquerque, New Mexico, USA

Correspondence to Matthew D. Neal, MD, Roberta G. Simmons Associate Professor of Surgery and Critical Care Medicine Department of Surgery, University of Pittsburgh School of Medicine, F1271.2 Presbyterian Hospital, 200 Lothrop St, Pittsburgh, PA 15213, USA
Tel: +1 412 647 1158; fax: +1 412 647 3389; e-mail: nealm@upmc.edu

Received 15 May 2021 **Revised** 30 August 2021
Accepted 6 September 2021

Introduction

Following traumatic injury, sympathoadrenal activation and loss of the vascular endothelial glycocalyx often lead to systemic endotheliopathy [1,2]. Damaged or activated vascular endothelium releases ultra-large von Willebrand factor (UL-vWF) from Weibel-Palade bodies [3–6]. In the acute phase of traumatic injury, the UL-vWF forms, which are known to have increased thrombotic and inflammatory potential, contribute to haemostasis [7,8]. However, it is unclear if persistence of these circulating high molecular weight multimeric-vWF (HMWM-vWF) forms result in organ injury or thrombotic complications. With increased vWF activity in traumatic injury, downstream pro-coagulant, thrombotic and inflammatory effects contribute to diseases such as trauma-induced coagulopathy, disseminated intravascular coagulation and systemic inflammatory response syndrome, as posited by studies evaluating critical illness states such as sepsis and burns [9]. Furthermore, specific effects of unregulated vWF activity are emphasized by the pathophysiology of thrombotic thrombocytopenic purpura (TTP), wherein vWF-dependent protease, ADAMTS13 (A Disintegrin and Metalloprotease with Thrombospondin Type 1 Motif 13), activity is drastically inhibited,

* Roberto I. Mota and Matthew D. Neal functioned as co-senior authors for this publication.

 DOI:10.1097/MBC.0000000000001089

Supplemental digital content is available for this article. Direct URL citations appear in the printed text and are provided in the HTML and PDF versions of this article on the journal's website (www.bloodcoagulation.com).

leading to acute kidney injury (AKI) due to microvascular depositions of pro-inflammatory and pro-thrombotic UL-vWF [10–14]. Interestingly, AKI is also common following traumatic injury, as it is reported to develop in up to 50% of traumatic injury patients [15–19]. However, although renal injury secondary to TTP is thought to be due to UL-vWF induced vascular damage, it is commonly accepted that the primary cause of trauma induced AKI is renal hypoperfusion due to shock [11–14]. We hypothesize that there is overlap between these two causes of AKI, and that the systemic endotheliopathy of trauma leads to microvascular depositions of UL-vWF.

Although recent work has evaluated the quantitative changes related to vWF and ADAMTS13 in critical illness states, the effects of persistent elevations of vWF activity in the circulation on organ injury remain incompletely explored. A recent study highlights the protective nature of recombinant human ADAMTS13 (rhADAMTS13) when given in a murine renal ischemia reperfusion model [20]. However, it is unclear whether there is a direct effect of vWF cleavage by ADAMTS13 that contributes to renal injury prevention, or whether there is simply a primary anti-inflammatory effect due to ADAMTS13. In essence, the effects of vWF that may lead to the renal injury following trauma are unexplored. Here, we seek to provide a preliminary assessment regarding changes in vWF form, antigen levels and collagen binding activity (CBA), along with renal histology, following traumatic injury in both humans and a murine model. These studies demonstrate downstream effects of vWF on the renal microvasculature and its potential contribution to renal injury.

Materials and methods

Trauma patient plasma and healthy control samples

Plasma samples were obtained from the PAMPer trial (Prehospital Air Medical Plasma trial) biorepository. The PAMPer trial is an IRB approved (PRO11120115) randomized control trial (NCT01818427) to study the effect of prehospital plasma resuscitation as compared with standard of care resuscitation in traumatic injury patients [21]. Briefly, patients enrolled in the PAMPer trial had at least one episode of hypotension (SBP <90 mmHg) as well as tachycardia (heart rate >108 beats per minute) or a single episode of severe hypotension (SBP <70 mmHg) prior to their arrival to a trauma centre. Plasma samples from the PAMPer trial were obtained from eight traumatic injury patients who developed AKI at time points, including 0 (upon admission), 24 and 72 h following severe traumatic injury. AKI was defined by at least 0.3 mg/dl increase in creatinine within 48 h of admission. The plasma samples from patients who developed AKI were well matched with trauma patients who did not develop AKI based upon age, injury severity score and lactate concentrations (Table 1).

The PAMPer trial was composed of a population of 523 patients. From this population, a total of 86 patients developed AKI as defined by the inclusion criteria in our analysis. A query of patients in this repository was performed with criteria, including development of AKI, availability of samples for at least two of the three timepoints of interest (0, 24 and 72 h), and ability to be

Table 1 Clinical demographics and values

Value	Non-AKI ($n=8$)	AKI ($n=8$)	Significance (P)
% Female:Male	12.5 : 87.5	25 : 75	–
Age	56 (49–63)	57 (50–64.5)	0.702
Injury Severity Score	19.5 (16.75–23.75)	23 (15.5–26.5)	0.899
GCS	8.5 (3–15)	10 (3–14.3)	0.915
% Blunt:Penetrating Injury:Both	87.5 : 12.5 : 0	50 : 37.5 : 12.5	–
Lowest SBP	76.5 (60.5–93.3)	81 (78.5–91.5)	0.513
Admission INR	1.3 (1.23–1.31)	1.21 (1.05–1.34)	0.899
Admission Creatinine	1.26 (1.08–1.52)	0.9 (0.89–1.05	0.010
Δ Creatinine (0–24 h)	−0.25 (−0.35–[−0.13])	0.5 (0.34–0.71)	0.0002
Admission Platelets	197 (177–265)	132 (104–182)	0.134
Admission Lactate	4.84 (2.9–5.9)	4.94 (3.0–6.2)	0.872
Units Prehospital Plasma Transfused	0 (0–1)	0 (0–0)	0.446
Units Blood Products Transfused in 24 h	7.5 (3–21)	12 (4.5–23.5)	0.702
Crystalloid in 24 h	9 (6.5–11)	8 (5.8–10.5)	0.740
Max BUN	16 (14.8–22)	25 (22–33.25)	0.170
% Receiving Prehospital Plasma	12.5	37.5	–
% On Aspirin / Antiplatelets	25	12.5	–
% On Anticoagulants	0	0	–
% On NSAIDs	25	37.5	–
% Smoker	12.5	12.5	–
% Hypertension Requiring Medication	62.5	25	–
% Diabetic	25	12.5	–
% PMH of Coagulopathy	0	0	–

Pertinent data are provided for the trauma patients who either did or did not develop secondary AKI with significance calculated where appropriate. Plasma samples were obtained from these groups and analysed in the following figures. Values reported as Median (IQR), unless otherwise stated.

matched for clinically important variables as noted above. This query of the biorepository of samples yielded $n = 8$ per group for a total of 16 patients. Of these patients, three (two in the AKI group and one in the non-AKI group) did not have plasma samples collected during the 72-h time point, and so data for these patients at the 72-h time point could not be included. Blood was drawn into citrate containing vacuum containers and platelet poor plasma was prepared from these samples. In addition to plasma from traumatic injury patients, plasma from seven healthy human controls were also drawn into citrate containing vacuum containers. Citrated pooled normal plasma (PNP) was purchased from George-King Biomedical to be used as a control. All plasma samples were stored at -80°C until use and thawed for 5 min in a 37°C water bath.

von Willebrand factor quantitative multimer analysis in human and murine plasma

Trauma patient or PNP samples were diluted in lithium dodecyl sulphate sample buffer (10 mmol/l Tris-HCl, 2% SDS, 2 mmol/l EDTA, 0.02% bromophenol blue and 43.5% glycerol, pH 6.8) to contain 0.6 μg/ml vWF. Samples were electrophoresed on a 1.5 mm, 1.75% vertical agarose gel at a constant current of 12.5 mA at 4°C. The gels were fixed, washed, blocked and stained with a 1 : 2000 dilution of primary polyclonal rabbit antihuman vWF (Dako, USA #A0082) or a 1 : 100 dilution of polyclonal rabbit antimouse vWF (ThermoFisher, USA #PA5-16634), followed by a 1 : 2000 dilution of secondary goat antirabbit IgG, Alexa Fluor 488 (ThermoFisher, USA #A-11008). A Bio-Rad Chemidoc MP Imager was used for fluorescent imaging, and Image Lab 6 was used to quantify lane and band fluorescence. To acquire percentage total lane fluorescence provided by HMWM-vWF forms, the total band volume of vWF more than 10 dimeric units (>5000 kDa) in length was divided by total lane fluorescence.

Human and murine ADAMTS13 activity, von Willebrand factor antigen, collagen binding activity and cystatin C ELISAs

'TECHNOZYM' ELISAs were purchased (Diapharma, USA #5450701, #5450201, #5450301 and MyBioSource, USA #MBS901541, #MBS2022796) to determine the circulating ADAMTS13 activity and antigen levels, vWF antigen and vWF CBA in plasma. Murine cystatin C ELISAs were purchased from Abcam (USA #ab201280). Murine and human plasma was generated by twice centrifuged citrated blood at 2000xg for 15 min.

Murine polytrauma and haemorrhagic shock model

Adult male C57Bl/6 mice were anesthetized with intraperitoneal pentobarbital sodium and inhaled isoflurane prior to our validated model of trauma and haemorrhage [22,23]. Approximately 30% (500 μl) of the total blood volume was rapidly removed into citrate within 1 min using a 1 ml syringe and a 30-gauge needle via closed cavity cardiac puncture. Previously prepared bone solution was injected bilaterally into the posterior muscles of each thigh at a volume of 0.15 ml using a 20-gauge needle. Soft tissue injury was performed using an 18-cm curved haemostat crushed with 270 psi on the bilateral lower extremities. A midline incision was made under the xyphoid, exposing the right middle lobe of the liver, which is crushed four times, at 80 psi, using a 12.5-cm curved haemostat. Laparotomy is closed, and animals are recovered for 120 min. Animals were sacrificed after either 24 or 72 h.

Murine kidney sectioning

Mouse kidneys were harvested during sacrifice at the 24-h timepoint of the polytrauma model. Kidneys were bisected and placed in 1x PBS pH 7.4 with 4% paraformaldehyde (PFA) fixative for 4 h at room temperature (RT). Kidneys were then washed, immersed and stored in sterile 1x PBS at 4°C. A Leica VT1000 S vibratome was used to cut 20 and 40-μm sections.

Murine kidney haematoxylin and eosin staining

Renal vibratome sections (20 μm) were plated and slides were immersed in gill II haematoxylin for 50 s, washed with water, immersed in bluing agent for 30 s, washed with water and then immersed in 95% ethanol, briefly. They were immersed in Eosin Y for 3–4 min followed by rinsing with water. Dehydration was performed using an ethanol wash. Slides were mounted using gelvatol and then visualized on a bright field microscope.

Murine kidney fluorescent staining

Renal vibratome sections (40 μm) were free float stained. Sections were permeabilized in 0.3% (v/v) Triton X-100 in 1x PBS at RT [24]. Sections were then blocked in 1x PBS with 0.2% (w/v) BSA and 0.3% (v/v) Triton X-100 at RT. Sections were stained with either 1 : 25 polyclonal rabbit antimouse vWF (ThermoFisher #PA5–16634) or 1 : 300 Sheep anti-Mouse Fibrinogen (Abcam #ab61352) in 1x PBS with BSA and Triton X-100 for 20-h at 37°C. Sections were washed and then immersed in 24 μg/ml Donkey anti-Sheep AlexaFluor 405 (Abcam #175676), in order to stain for fibrinogen, or Goat anti Rabbit Alexa-Fluor 647 (ThermoFisher #A32733), in order to stain for vWF, for 4 h in a 37°C oven. Sections were washed and then immersed in 200 μg/ml wheat germ agglutinin, Alexa Fluor 488 conjugate (ThermoFisher, USA #W11261) for 30 min at 37°C, to stain for nonspecific renal structure. Sections were washed, dehydrated, mounted in gelvatol and imaged on a Fluoview FV1000 Confocal Microscope. In the generation of secondary controls, the same protocol was utilized, but antibodies were excluded during the primary antibody incubation step.

Total liver RNA isolation and qRT-PCR analysis

Mouse liver (60 mg) was obtained at 0 (immediately before), 24 or 72 h during a polytrauma model. Samples taken from the 24 or 72-h time points were obtained from the lobe of the liver that was not injured at 0 h. The livers were immediately immersed and blended in 1 ml of TRI Reagent (Sigma #T9424) on ice. Total liver RNA isolation proceeded according to the manufacturer's protocol. A SuperScript III First-Strand Synthesis SuperMix for qRT-PCR (ThermoFisher #11752050) was utilized to produce cDNA. qRT-PCR was performed using a Lightcycler 96 System with PowerUp SYBR Green Master Mix according to the provided protocol. A 12-specific sense primer (5' – TCCTTCTACCACTGGGATGC – 3') and a 13-specific antisense primer (5' – TCCTTCTACCACTGGGATGC – 3') were utilized at 500 nmol/l concentrations to amplify the murine ADAMTS13 sequence [25]. A murine GAPDH primer pair was purchased as a housekeeping gene (Origene #MP205604) and data were normalized with respect to GAPDH expression.

LX-2 culture and hypoxia model

LX-2 immortalized human hepatic stellate cell line was procured from (Millipore Sigma, USA SCC064). Cells were grown to 60% confluency at 37°C in high glucose Dulbecco's Modified Eagle Medium with supplemented penicillin-streptomycin and L-glutamine. Cells were transferred to a hypoxia chamber where they were either incubated for 1.5 or 3 h at 37°C and 1% oxygen. Cells were then either harvested or allowed to incubate in a normoxic incubator for 1 or 3 h. Following this final incubation period, cells were harvested and prepared for qRT-PCR analysis as above.

Statistical analysis

Prism 8 for Mac (Graphpad Prism) was utilized for statistical analyses. One-to-one comparative studies were performed with the built-in Mann–Whitney *U* function or Wilcoxon Signed Rank. Correlative analyses were executed using the built-in linear regression tool and Spearman Correlation analysis. Given the exploratory nature of this analysis, a multiple comparisons correction was not utilized [26]. Data are presented as median ± interquartile range. A threshold for significance was defined as P value less than 0.05.

Results

HMWM-vWF increases in trauma patients who develop acute kidney injury and is associated with ADAMTS13 activity

HMWM-vWF was elevated at all time points for all traumatic injury patients when compared with control healthy plasma samples (Fig. 1a and b). At the 72-h time point, patients who developed AKI demonstrated significantly elevated HMWM-vWF forms, when compared with non-AKI counterparts [32.9% (30.4–35.3) vs. 27.8% (24.6–30.8) $P = 0.02$] (Fig. 1b). A significant inverse relationship was generated when plotting HMWM-vWF composition against ADAMTS13 activity from all traumatic injury samples ($r = -0.35$, $P = 0.018$) (Fig. 1c). Representative plots for separate time points, including 0, 24 and 72 h, may be found in supplemental Figure 1A, http://links.lww.com/BCF/A113.

vWF antigen levels from patients with traumatic injury, regardless of renal function, showed sustained elevation at the 0 to 72-h time points when compared with healthy controls [Combined 0–72 h data: 12.4 μg/ml (10.6–13.6) vs. 4.5 μg/ml (3.3–5.1) $P < 0.0001$] (Fig. 2a). Patients who developed AKI had a statistically significant increase in vWF levels between the 0 and 72-h time points [9.42 μg/ml (6.1–12.4) vs. 14.23 μg/ml (12.6–15.4) $P = 0.016$] (Fig. 2a). ADAMTS13 activity levels in both AKI and non-AKI traumatic injury patients were consistently lower at all time points when compared with healthy controls [Combined 0–72 h data: 0.47 IU/ml (0.44–0.58) vs. 1.29 IU/ml (1.13–1.60) $P < 0.0001$] (Fig. 2b). Evaluation of vWF Antigen:ADAMTS13 activity ratio between control trauma patients and those who developed AKI demonstrated no significant difference at the 0 and 24-h time points [0 h: 28.1 (20.2–36.9) vs. 22.3 (16.5–34.3), 24 h: 24.0 (18.5–32.4) vs. 25.8 (17.8–34.7)]. However, at the 72-h time point, a significant difference was seen in the vWF Antigen:ADAMTS13 activity ratio between control trauma patients and trauma patients who developed AKI [29.3 (18.6–33.9) vs. 37.8 (34.6–41.8) $P = 0.02$] (Fig. 2c).

vWF collagen binding activity

vWF antigen levels strongly correlated with type III CBA of samples from 0 to 72 h ($r = 0.83$, $P < 0.0001$) (Fig. 2d), indicating that the circulating vWF antigen demonstrated prothrombotic activity in proportion with its concentration. The ADAMTS13 activity level was inversely related to CBA:vWF antigen ratio for samples at 24 and 72 h ($r = -0.46$, $P = 0.01$) (Fig. 2e). The red dotted line in Fig. 2e represents the median CBA:vWF antigen ratio of healthy control samples, which was markedly lower when compared to all trauma samples [0.166 IU/ml:μg/ml (0.149–0.202)] vs. 0.212 IU/ml:μg/ml (0.188–0.247) $P < 0.01$]. Representative plots for separate time points, including 0, 24 and 72 h, for Fig. 2d and e may be found in supplemental Figure 1B and 1C, http://links.lww.com/BCF/A113, respectively.

Murine trauma and haemorrhagic shock is associated with vWF form and renal function

Analysis of plasma samples from each mouse at 0, 6 and 24 h showed a significant increase in cystatin C levels [496 ng/mL (439–575) vs. 640 ng/ml (552–709) vs. 550 ng/ml (493–701), $P < 0.001$ and $P = 0.02$, respectively] (Fig. 3a), suggesting inhibited renal function [27,28]. Figure 3b demonstrates that mice had elevated cystatin C at both 6 and 24 h when compared with baseline.

Fig. 1

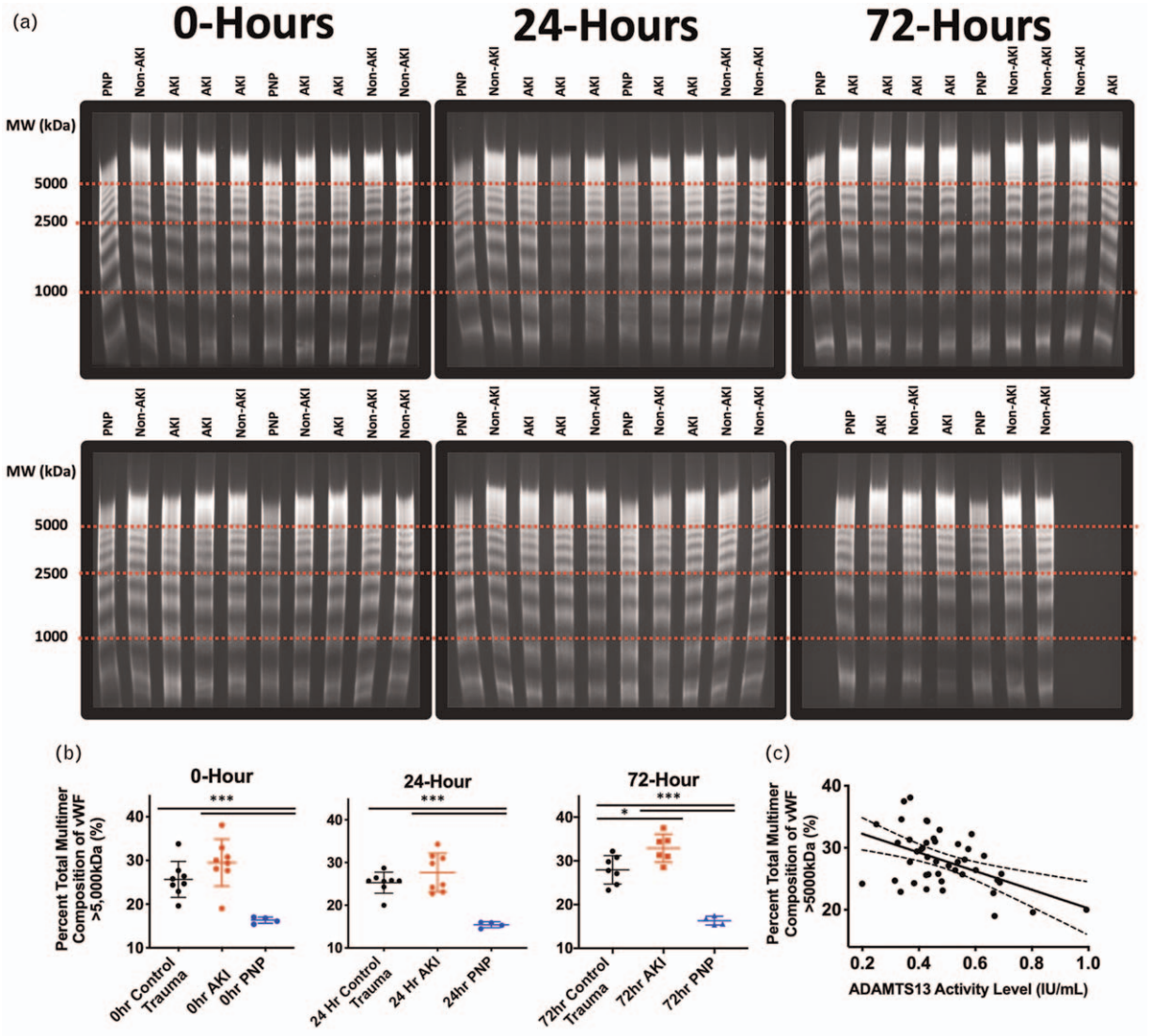

High molecular weight multimeric vWF is elevated in patients who develop post-traumatic acute kidney injury. (a) vWF multimeric form was evaluated by means of 1.75% vertical agarose gel electrophoresis. Each lane evaluates a single traumatic injury patient who did or did not develop AKI; the red dotted lines denote various molecular weight (MW) cutoffs. (b) Patients who developed AKI demonstrated significantly elevated HMWM vWF forms, when compared to non-AKI counterparts, 72 h after injury [32.9% (30.4–35.3) vs. 27.8% (24.6–30.8) P.0.02]. (c) A significant inverse relationship is generated when plotting HMWM-vWF composition against ADAMTS13 activity of all trauma samples (Spearman $r = -0.35$, P=0.018).

Figure 3c and d illustrate that murine plasma vWF antigen levels rose [0 h = 18.0 μg/ml (11.6–22.8) vs. 6 h = 26.5 μg/ml (23.4–36.9] vs. 24 h = 63.7 μg/ml (59.9–81.0) $P < 0.0001$], while murine ADAMTS13 levels decreased significantly [0 h = 0.200 μg/ml (0.167–0.255) vs. 6 h = 0.146 (0.118–0.175) $P < 0.001$ vs. 24 h = 0.102 (0.066–0.163) $P < 0.0001$].

Notably, a significant inverse relationship was seen: polytrauma mice with lower ADAMTS13 demonstrated increased vWF antigen levels [spearman $r = -0.49$ (−0.75 to −0.08 $P = 0.01$)] (Fig. 3e). Of note, the median murine vWF antigen:ADAMTS13 antigen ratio significantly increased at each time point [0 h = 0.14 (0.06–0.45) vs. 6 h = 0.56 (0.44–0.63) vs. 24 h = 0.8 (0.75–0.89), with all $P < 0.003$] (Data not shown). Furthermore, similar to human trauma patients, the murine polytrauma model also demonstrated increased vWF multimeric forms circulating within their plasma at the 6-h time point (lanes labelled 'post'), when compared to the 0-h time point (lanes labelled 'pre') [34.8% (29.0–36.1) vs. 30.0% (25.9–32.61) $P = 0.01$] (Fig. 3f and g). Unedited versions of the gels in Fig. 3g may be found in Supplemental Figure 2, http://links.lww.com/BCF/A114.

Fig. 2

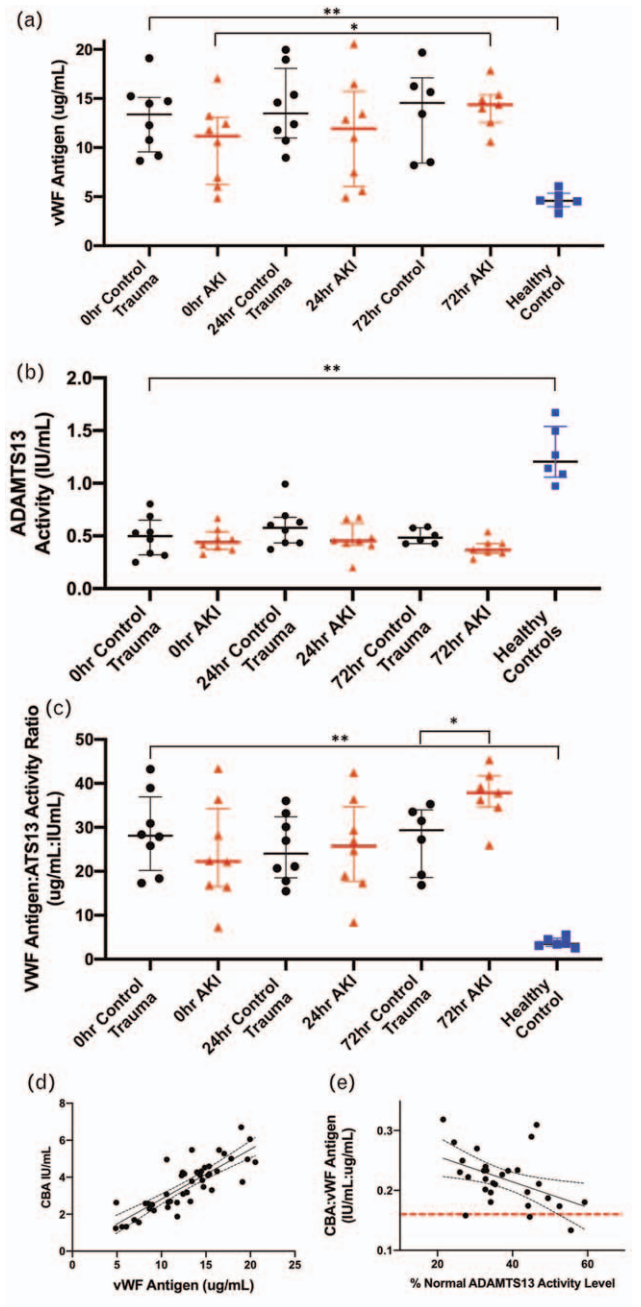

vWF and ADAMTS13 levels in patients suffering traumatic injury. (a,b) vWF levels of both AKI and non-AKI traumatic injury patients at 0-, 24-, and 72-h time points compared to healthy controls ([Healthy Control: 4.57mg/ml (3.99–5.35)], [ControlTrauma (Non-AKI) 0 h: 13.37mg/ml (9.56–15.11), 24 h: 13.48mg/ml (10.98–18.07), 72 h: 14.54mg/ml (8.43–17.11)], [AKI Patient 0 h: 11.18mg/ml (6.28–11.18), 24 h: 11.93mg/ml (6.05–15.72), 72 h: 14.36mg/ml (12.58–15.35)]. ADAMTS13 activity levels of both AKI and non-AKI traumatic injury patients at 0-, 24-, and 72-h time points compared to healthy controls ([Healthy Control: 1.3 IU/ml (1.06–1.53)], [Control Trauma (Non-AKI) 0 h: 0.50 IU/ml (0.32–0.65) 24 h: 0.58 IU/mL (0.43–0.68) 72 h: 0.48 IU/ml (0.43–0.58), [AKI Patient 0.44 IU/ml (0.37–0.54) 24 hr: 0.57 IU/ml (0.43–0.68) 72 h: 0.37 IU/ml (0.34–0.43)]. (c) vWF Antigen:ADAMTS13 Activity Ratio of control trauma patients was significantly different than those that developed AKI at the 72-h time point [29.3 (18.6–33.9) vs. 37.8 (34.6–41.8) P.0.02]. (d) vWF Antigen levels strongly correlated with type III collagen binding assay (CBA) activity of samples from 0 to 72 h (r=0.83, P<0.0001). (e) The ADAMTS13 activity level was inversely related to CBA:vWF antigen ratio for samples from 24 and 72 h (r= −0.46, P.0.01). The red dotted line represents the median CBA:vWF Antigen ratio of healthy control samples [0.166IU/ml:μg/ml (0.149-0.202)].

ADAMTS13 expression following murine polytrauma model and in-vitro hypoxia models

ADAMTS13 gene expression in total liver RNA decreased within 24-h post murine polytrauma model injury, with a significant rebound at 72 h [1.00 (0.98–1.02) vs. 0.42 (0.36–0.56), $P \leq 0.01$ and 0.42 (0.36–0.56) vs. 0.62 (0.55–0.71), $P = 0.04$] (See Supplemental Methods and Supplemental Fig 3A, http://links.lww.com/BCF/A115). When LX-2 hepatic stellate cells underwent a 1.5-h incubation in a 1% hypoxia chamber, there was a significant decrease in *ADAMTS13* gene expression and this level was sustained at the 3-h time point [1.00 (0.98–1.02) vs 0.70 (0.64–0.78), $P = 0.03$ and 0.70 (0.64–0.78) at 1.5 h, and 0.69 (0.63–0.77) at 3 h, $P = 0.99$ when compared with 1.5 h] (See Supplemental Methods and Supplemental Fig 3B, http://links.lww.com/BCF/A115). When returned to a normoxic incubator for 3 h, a significant rebound in ADAMTS13 gene expression was seen in the cells that underwent a 1.5-h hypoxic insult [0.70 (0.64–0.78) vs. 0.94 (0.87–0.98), $P = 0.03$]. However, cells that had been incubated in hypoxic conditions for 3 h showed a persistent reduction in *ADAMTS13* gene expression [0.69 (0.63–0.77) vs. 0.71 (0.66–0.73), $P = 0.99$].

Histologic evaluation of renal architecture

Analysis of the cortical region of 20 μm PFA fixed kidney sections by haematoxylin and eosin staining (H&E) showed marked differences between healthy mice and those that underwent a polytrauma model. Major variations between these samples may be seen at both 20x and 40x optics (Fig. 4a). Notably, the traumatic injury sections showed loss of tubular lumen structure with dilation of tubules and denudation of tubular cells in the cortical region (black arrows). These effects became most prominent in mice demonstrating more than 200 ng/ml increase in cystatin C following traumatic injury (Fig. 4a, right).

We used 40 μm PFA fixed kidney sections and free float stained them for fibrinogen (blue channel, Alexa Fluor 647), vWF (red channel, Alexa Fluor 405) or sialic acid and N-acetylglucosaminyl residues for general structure [green channel, using wheat germ agglutinin Alexa Fluor-488 conjugate (WGA-488)]. A healthy kidney section evaluated with both a 20x and 100x optic showed normal architecture (Fig. 4b). Evaluation of the small vessel vasculature demonstrated clear vessel lumens, despite regions with weak, strand-like fibrinogen staining. VWF (red) was seen clustered in endothelial cells surrounding tubules.

Twenty-four hour post polytrauma model, dilated tubules with denuded cells were seen under the 20x

Fig. 3

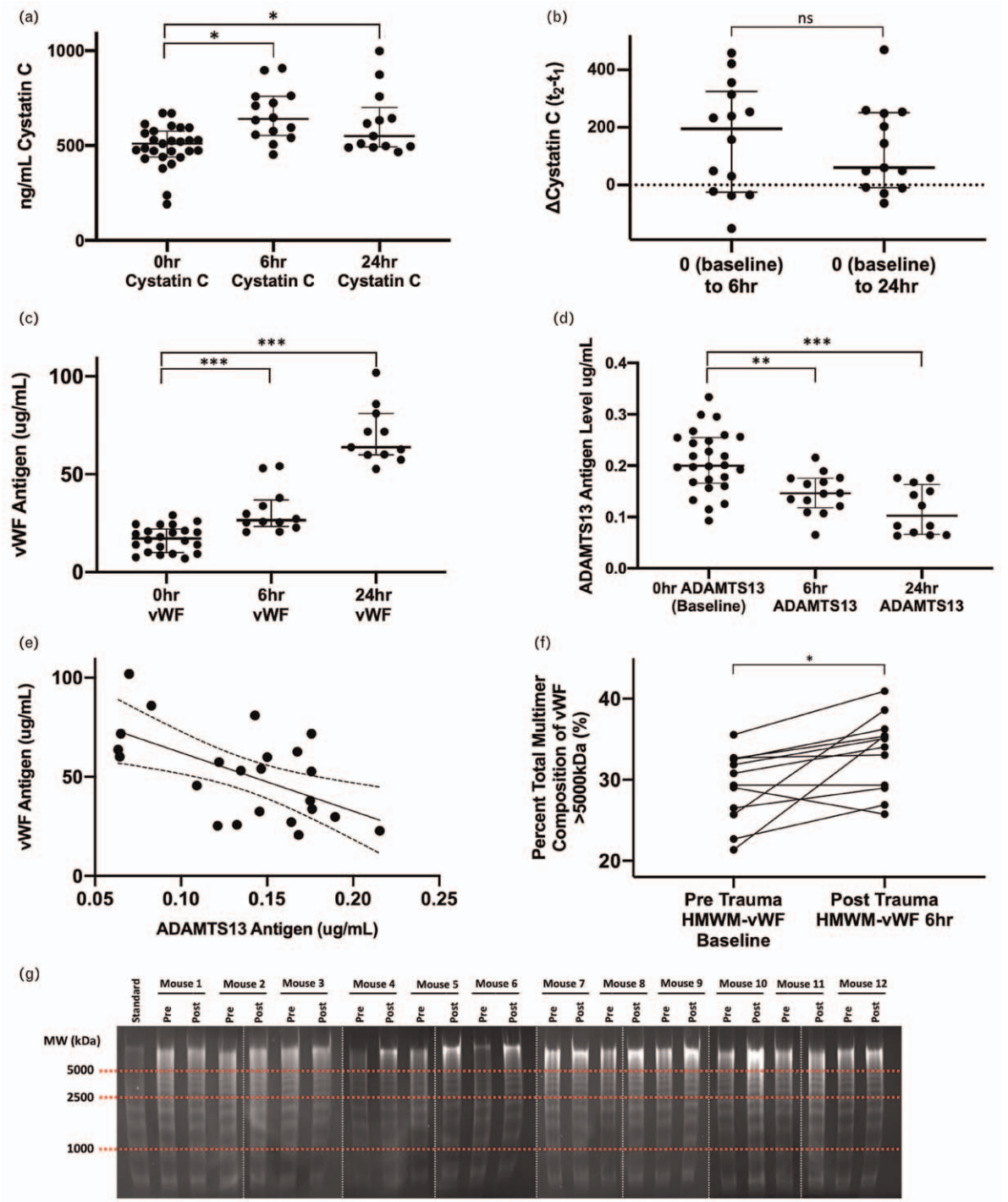

Haematological and renal effects of a murine polytrauma model. Mice underwent a polytrauma model. (a,b) Plasma samples from mice demonstrated a significant increase in cystatin C levels over 6 and 24-h post polytrauma model [496 ng/ml (439–575) vs. 553 ng/ml (479–640) vs. 550 ng/ml (466–701)]. (c) vWF levels showed significant increases over this 24-h time period as well [0 h = 18.0 μg/ml (11.6–22.8) vs. 6 h = 26.5 μg/ml (23.4–36.9) $P < 0.0001$ vs. 24 h = 63.7 μg/ml (59.9–81.0)]. (d) ADAMTS13 antigen decreased following the murine polytrauma model [0 h = 0.200 μg/ml (0.167–0.255) vs. 6 h = 0.146 (0.118–0.175) $P < 0.001$ vs. 24 h = 0.102 (0.066–0.163) $P < 0.0001$]. (e) There was a significant inverse relationship between murine ADAMTS13 antigen levels and vWF antigen levels pooled from both 6 and 24 h post polytrauma model [spearman $r = -0.49$ (−0.75 to −0.08) $P = 0.02$]. (f,g) A matched analysis of murine HMWM-vWF forms demonstrated significant increases 6hrs following the polytrauma model [30.0% (25.9–32.61 vs. 34.8% (29.0–36.1)]. Two lanes were utilized for each mouse, denoted above the gels as 'pre' or 'post' traumatic injury, which refer to plasma samples obtained immediately prior to injury ('pre') or 6hrs after injury ('post'). Horizontal red dotted lines designate various MW cutoffs. Vertical white dotted lines indicate cropped standard lanes.

Fig. 4

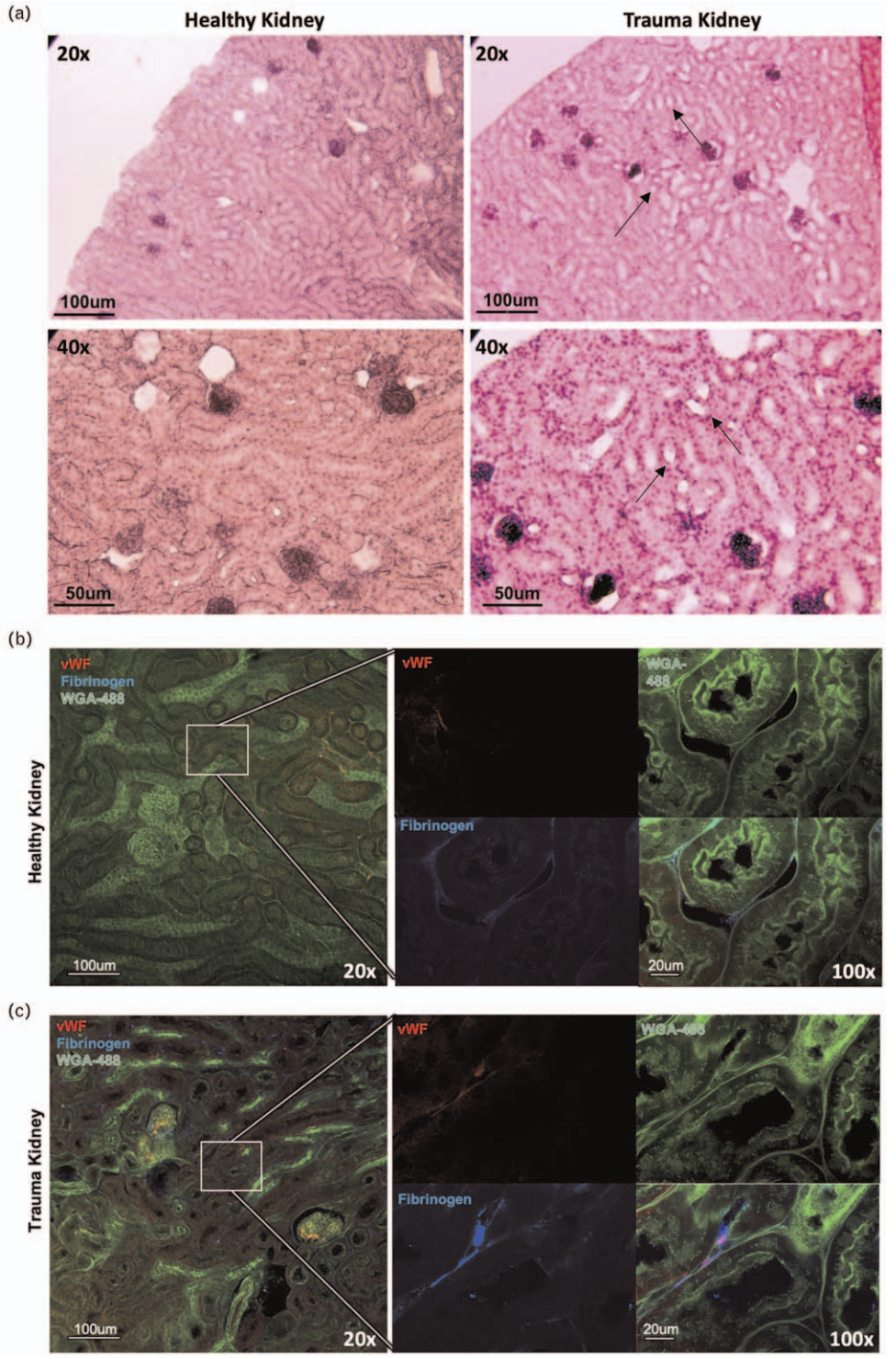

Murine histologic and immunohistochemical vWF deposition analysis. (a) Left: H&E slide showing a 20um thick PFA fixed healthy kidney section with both 20x and 40x optics. Right: H&E slide demonstrating a 20um thick PFA fixed kidney section from a mouse with a >200 ng/ml increase in cystatin C following traumatic injury. Note dilated lumens with denudation of tubule cells (Black Arrows). (b) A 20x optic, healthy kidney section with a 100x optic blow out of generalized small vessels utilizing RGB-colour channels is shown. vWF is shown utilizing red, fibrinogen with blue, and generalized structure using green. Weak fibrinogen staining can be seen within the vessel lumen. (c) A 20x optic, 24-h post polytrauma model kidney section is shown. Under the 100x optic, small vessel plugs are visible, staining strongly for fibrinogen with a central region containing vWF; this overlap appears purple within the images.

fluorescent optic (Fig. 4c). Under the 100x optic, small vessel plugs were visible, staining strongly for fibrinogen (blue) with a central region containing vWF (red); this overlap appears purple within the combined images. Relevant secondary controls are provided in Supplemental Figure 4, http://links.lww.com/BCF/A116, demonstrating a lack of nonspecific, red or blue secondary antibody staining.

Discussion

With this work, our group provided evidence regarding potential contributions of vWF in the development of AKI secondary to traumatic injury. Microvascular depositions of vWF appeared in mice that developed AKI, but these depositions were not seen in those that did not develop AKI. These findings suggested that vWF was not only acting as an acute phase reactant, but also as a direct contributor to renal injury. Given these data, we posit that the environment that is generated following traumatic injury, when paired with increased HMWM-vWF forms and an increased vWF:ADAMTS13 ratio, exacerbates renal injury through the demonstrated deposition of proinflammatory vWF-containing small vessel plugs [10,16,29–32].

Trauma patient plasma samples demonstrated a threefold increase in vWF antigen upon admission. As the 72-h time point approached, those patients that developed AKI trended towards having increased vWF antigen and percentage composition of HMWM-vWF (Figs. 1b and 2a). There were no significant differences in vWF antigen or ADAMTS13 levels between those who did or did not develop AKI at any time point (Fig. 2a and b). However, significant increases were seen in vWF:ADAMTS13 in the AKI patients at the 72-h time point, when compared with controlled trauma patients. These data suggested that although there were similar values of vWF antigen and ADAMTS13 activity separately, the combined effect of these changes may markedly contribute to a prothrombotic environment within patients that develop AKI (Fig. 2c).

Although the data from human trauma plasma samples showed significant changes in ADAMTS13 and vWF form and function following traumatic injury, the study was limited in its ability to be generalized by the sample size of eight patients per arm. Importantly, while 523 patients met inclusion criteria for the original PAMPer trial, there were eight total patients who developed AKI that had plasma samples from at least two out of three of the necessary time points (0, 24 and 72 h), and were also able to be well matched according to age, injury severity score and lactate (Table 1). Notably, of the samples that were obtained for our study, we were unable to control for the administration of prehospital plasma. Only four of the 16 patients in this cohort received prehospital plasma (three who developed AKI, one who did not). Although this may have minimally affected the 0-h time point, the number of transfused units of blood products between both patient groups were equivalent by the 24-h time point (Table 1). These data suggested that the effect of blood product transfusion on later time points was likely equivalent between AKI and non-AKI patients.

The small study population likely inhibited our ability to detect small effect sizes, such as differences in vWF multimeric form (Fig. 1b). Unfortunately, vWF agarose gel electrophoresis is intrinsically limited by its low throughput protocol. Although the limitation of small sample size does confound our ability to broadly extrapolate these data, it was adequate for the purposes of supporting the preliminary nature of this work. Future studies will need to examine potential for updating methods of vWF multimeric analysis towards a protocol that allows for higher throughput of multimer approximation, which would allow for the assessment of larger sample sizes.

A well defined murine polytrauma model was utilized in order to evaluate if mice demonstrated posttraumatic pathologic similarities in ADAMTS13 and vWF, when compared with humans. The incidence of animals demonstrating a more than 200 ng/ml increase in cystatin C was 50% at 6 h and 38% at 24 h (Fig. 3a and b); furthermore, these samples demonstrated signs of acute tubular necrosis when evaluated microscopically (Fig. 4a), suggesting that severe renal injury was being produced at rates similar to typical traumatic injury patients [15–19,33,34]. Unfortunately, in-depth analyses that define a relationship between AKI and cystatin C levels in mice are lacking. However, Leelahavanichkul *et al.* [27] provided important insights in their work, which demonstrated that acute increases in cystatin C suggest a drastically reduced inulin glomerular filtration rate, and thus renal injury. Although serum creatinine levels would have circumvented the need for cystatin C measurements, low circulating serum levels were undetectable by our ELISAs. Furthermore, murine urine, which typically holds a higher concentration of creatinine than murine serum, was not consistently obtainable at the time of sacrifice.

Given that ADAMTS13 antigen levels were lower in both mice and humans following traumatic injury (Fig. 2b), the effect of traumatic injury on hepatic ADAMTS13 mRNA production was evaluated, as the liver is described as a major ADAMTS13 producing organ (Supplemental Figure 3A, http://links.lww.com/BCF/A115) [25]. These studies were performed in order to understand if the mice compensated for the decreases in circulating ADAMTS13 antigen by means of upregulating production of *ADAMTS13* gene expression. ADAMTS13 RNA expression levels were inhibited by 60% at the 24-h time point following traumatic injury (Supplemental Fig 3A, http://links.lww.com/BCF/A115). We hypothesized that the lack of ADAMTS13 mRNA

production may be a consequence of the ischemic insult, due to shock, following traumatic injury (Supplemental 3B, http://links.lww.com/BCF/A115) [35], along with cytokine release as previously demonstrated [36]. To fully understand the effects traumatic injury on the production of ADAMTS13, it would be necessary to evaluate other sources of ADAMTS13, such as the vascular endothelium [37]. Given the highly vascularized nature of the liver, we were limited in our analysis, as we were unable to identify if the ADAMTS13 mRNA that we detected in total liver RNA was sourced from hepatic stellate cells or from vasculature. However, the in-vitro, hypoxic LX-2 hepatic stellate cell exposure model (Supplemental Fig 3B, http://links.lww.com/BCF/A115) suggested a potential role for hypoxic inhibition of stellate cell ADAMTS13 RNA production, which was previously unrecognized.

To evaluate if there was a distribution of the circulating murine vWF within the kidney, we assessed renal architecture by microscopy (Fig. 4) [24,38]. Diffuse staining of endothelial vWF, was present in kidneys of both healthy and traumatically injured mice. Importantly, the kidneys in the traumatically injured mice showed evidence of vWF and fibrinogen containing microvascular plugs, measuring from 8 to 16 μm in size, which were unapparent in uninjured mice (Fig. 4c). The structure of these plugs showed a weaker vWF staining center with a strong fibrinogen staining overlap, which is conducive with typical clot structure (Fig. 4c) [39]. Notably, the form of circulating vWF and the environment it is exposed to are likely primary predictors of the rate at which these vWF-containing microvascular plugs form, as vWF binding to either the sub-endothelium or the endothelium is the driver of platelet adherence in thrombus formation [40,41]. Future studies would benefit from contrasting the molecular structure of thrombi seen in our traumatic injury mouse model to those generated in a murine TTP model [42–44]. The demonstration of similarly structured vWF rich thrombi in both mouse models would further support the primary role of vWF in the production of these thrombi.

Although we did demonstrate similarities between our mouse model with the human trauma patients that were studied, our ability to translate our results from one group to another was hindered by variations in ADAMTS13 and vWF antigen levels, form, and function in mice when compared with humans. These shortcomings were rectified by the functional demonstration of the prothrombotic high molecular weight vWF forms that may have led to the microvascular deposits that were seen on renal microscopy. However, future studies are warranted to evaluate for the ability to clear vWF from the renal microvasculature, by means of recombinant ADAMTS13 administration, in an attempt to prevent the development of AKI. Recent evidence suggested that rhADAMTS13 may reduce the burden of shock and organ injury in a rat transfusion model [45]. Aspects such as route and timing of administration of ADAMTS13 will require extensive calibrations. Furthermore, either recombinant murine ADAMTS13 or extensive characterization of recombinant human ADAMTS13 on mice will be needed in order to evaluate specificity and mechanisms of its effects. These further studies were not within the scope of our current project, which sought to demonstrate the fate of an increasingly pro-thrombotic and pro-inflammatory population of vWF on the renal circulation.

Our group has shown that traumatic injury causes drastic variations within circulating vWF form and function. Concomitantly, ADAMTS13 levels plummet, perhaps becoming unable to control the circulating vWF population. The pathological state of trauma leads to conditions that can exacerbate renal injury, not only including hypoperfusion due to shock, but also deposition of microvascular plugs due to variations in vWF and ADAMTS13. We conclude that trauma shifts the vWF-ADAMTS13 axis towards a prothrombotic state by means of alterations in circulating factors such as an elevated vWF:ADAMTS13 ratio and increased prothrombotic HMWM-vWF. Ultimately, we believe these changes may contribute to trauma induced renal injury by increasing the risk for microvascular thrombotic events.

Acknowledgements

We would like to thank Dr. Catherine J. Baty at the Renal-Electrolyte Division of the University of Pittsburgh School of Medicine for her expertise in renal imaging.

W.E.P., S.H.H., M.R.D., M.A.R., J.S.R., B.S.Z. and M.D.N. designed the study. W.E.P. and S.H.H. performed all experiments. W.E.P., S.H.H., P.A.L., J.A., A.H., L.H., N.A., R.I.M. and M.D.N. analysed the data. J.L.S. and F.X.G. provided human samples for analysis and critical review of the manuscript. W.E.P., R.I.M. and M.D.N. wrote the manuscript.

Funding was provided by 1R35GM119526-01 and R01HL141080-01A1 to M.D.N., UM1HL120877 to J.L.S., B.S.Z. and M.D.N., W81XWH-12-2-0023 to F.X.G. and J.L.S., 5T32GM008516 to M.R.D., Carolyn L. Kuckein Student Research Fellowship from Alpha Omega Alpha to W.E.P.

Conflicts of interest

M.D.N. has the following financial relationships to disclose: Consultant, External Scientific Advisor for Anticoagulation Science for Janssen Pharmaceuticals (Johnson & Johnson), Research funding from Haemonetics and Instrument Laboratories, Scientific Advisory Board of Haima Therapeutics, Trauma Advisory Board, CSL Behring and US Patent 9,072,760 *TLR4 inhibitors for the treatment of human infectious and inflammatory disorders* (issued to Neal, Wipf, Hackam, Sodhi). The additional authors declare that no significant conflicts of interest exist.

References

1 Johansson PI, Stensballe J, Ostrowski SR. Shock induced endotheliopathy (SHINE) in acute critical illness: a unifying pathophysiologic mechanism. *Crit Care* 2017; **21**:25.

2 Ostrowski SR, Henriksen HH, Stensballe J, Gybel-Brask M, Cardenas JC, Baer LA, *et al.* Sympathoadrenal activation and endotheliopathy are drivers of hypocoagulability and hyperfibrinolysis in trauma: a prospective observational study of 404 severely injured patients. *J Trauma Acute Care Surg* 2017; **82**:293–301.

3 Claus RA, Bockmeyer CL, Budde U, Kentouche K, Sossdorf M, Hilberg T, *et al.* Variations in the ratio between von Willebrand factor and its cleaving protease during systemic inflammation and association with severity and prognosis of organ failure. *Thromb Haemost* 2009; **101**:239–247.

4 Ono T, Mimuro J, Madoiwa S, Soejima K, Kashiwakura Y, Ishiwata A, *et al.* Severe secondary deficiency of von Willebrand factor-cleaving protease (ADAMTS13) in patients with sepsis-induced disseminated intravascular coagulation: its correlation with development of renal failure. *Blood* 2006; **107**:528–534.

5 Bagshaw SM, George C, Gibney RT, Bellomo R. A multicenter evaluation of early acute kidney injury in critically ill trauma patients. *Ren Fail* 2008; **30**:581–589.

6 Sandsmark DK, Bogoslovsky T, Qu BX, Haber M, Cota MR, Davis C, *et al.* Changes in plasma von Willebrand factor and cellular fibronectin in MRI-defined traumatic microvascular injury. *Front Neurol* 2019; **10**:246.

7 Luo GP, Ni B, Yang X, Wu YZ. von Willebrand factor: more than a regulator of hemostasis and thrombosis. *Acta Haematol* 2012; **128**: 158–169.

8 Kumar MA, Cao W, Pham HP, Raju D, Nawalinski K, Maloney-Wilensky E, *et al.* Relative deficiency of plasma A disintegrin and metalloprotease with thrombospondin Type 1 repeats 13 activity and elevation of human neutrophil peptides in Patients with traumatic brain injury. *J Neurotrauma* 2019; **36**:222–229.

9 Habe K, Wada H, Ito-Habe N, Hatada T, Matsumoto T, Ohishi K, *et al.* Plasma ADAMTS13, von Willebrand factor (VWF) and VWF propeptide profiles in patients with DIC and related diseases. *Thromb Res* 2012; **129**:598–602.

10 Tsai HM. Pathophysiology of thrombotic thrombocytopenic purpura. *Int J Hematol* 2010; **91**:1–19.

11 Eriksson M, Brattstrom O, Martensson J, Larsson E, Oldner A. Acute kidney injury following severe trauma: risk factors and long-term outcome. *J Trauma Acute Care Surg* 2015; **79**:407–412.

12 Shashaty MG, Meyer NJ, Localio AR, Gallop R, Bellamy SL, Holena DN, *et al.* African American race, obesity, and blood product transfusion are risk factors for acute kidney injury in critically ill trauma patients. *J Crit Care* 2012; **27**:496–504.

13 Skinner DL, Hardcastle TC, Rodseth RN, Muckart DJ. The incidence and outcomes of acute kidney injury amongst patients admitted to a level I trauma unit. *Injury* 2014; **45**:259–264.

14 Elterman J, Zonies D, Stewart I, Fang R, Schreiber M. Rhabdomyolysis and acute kidney injury in the injured war fighter. *J Trauma Acute Care Surg* 2015; **79**:S171–S174.

15 Lopes JA, Jorge S, Resina C, Santos C, Pereira A, Neves J, *et al.* Acute kidney injury in patients with sepsis: a contemporary analysis. *Int J Infect Dis* 2009; **13**:176–181.

16 Perkins ZB, Captur G, Bird R, Gleeson L, Singer B, O'Brien B. Trauma induced acute kidney injury. *PLoS One* 2019; **14**:e0211001.

17 Alobaidi R, Basu RK, Goldstein SL, Bagshaw SM. Sepsis-associated acute kidney injury. *Semin Nephrol* 2015; **35**:2–11.

18 Heegard KD, Stewart IJ, Cap AP, Sosnov JA, Kwan HK, Glass KR, *et al.* Early acute kidney injury in military casualties. *J Trauma Acute Care Surg* 2015; **78**:988–993.

19 Lai WH, Rau CS, Wu SC, Chen YC, Kuo PJ, Hsu SY, *et al.* Posttraumatic acute kidney injury: a cross-sectional study of trauma patients. *Scand J Trauma Resusc Emerg Med* 2016; **24**:136.

20 Zhou S, Jiang S, Guo J, Xu N, Wang Q, Zhang G, *et al.* ADAMTS13 protects mice against renal ischemia-reperfusion injury by reducing inflammation and improving endothelial function. *Am J Physiol Renal Physiol* 2019; **316**:F134–F145.

21 Sperry JL, Guyette FX, Brown JB, Yazer MH, Triulzi DJ, Early-Young BJ, *et al.* Prehospital plasma during air medical transport in trauma patients at risk for hemorrhagic shock. *N Engl J Med* 2018; **379**:315–326.

22 Vogel S, Bodenstein R, Chen Q, Feil S, Feil R, Rheinlaender J, *et al.* Platelet-derived HMGB1 is a critical mediator of thrombosis. *J Clin Invest* 2015; **125**:4638–4654.

23 Dyer MR, Alexander W, Hassoune A, Chen Q, Brzoska T, Alvikas J, *et al.* Platelet-derived extracellular vesicles released after trauma promote hemostasis and contribute to DVT in mice. *J Thromb Haemost* 2019; **17**:1733–1745.

24 Smyrek I, Stelzer EH. Quantitative three-dimensional evaluation of immunofluorescence staining for large whole mount spheroids with light sheet microscopy. *Biomed Opt Express* 2017; **8**:484–499.

25 Zhou W, Inada M, Lee TP, Benten D, Lyubsky S, Bouhassira EE, *et al.* ADAMTS13 is expressed in hepatic stellate cells. *Lab Invest* 2005; **85**:780–788.

26 Althouse AD. Adjust for multiple comparisons? It's not that simple. *Ann Thorac Surg* 2016; **101**:1644–1645.

27 Leelahavanichkul A, Souza AC, Street JM, Hsu V, Tsuji T, Doi K, *et al.* Comparison of serum creatinine and serum cystatin C as biomarkers to detect sepsis-induced acute kidney injury and to predict mortality in CD-1 mice. *Am J Physiol Renal Physiol* 2014; **307**:F939–F948.

28 Song S, Meyer M, Turk TR, Wilde B, Feldkamp T, Assert R, *et al.* Serum cystatin C in mouse models: a reliable and precise marker for renal function and superior to serum creatinine. *Nephrol Dial Transplant* 2009; **24**:1157–1161.

29 Legrand M, Bezemer R, Kandil A, Demirci C, Payen D, Ince C. The role of renal hypoperfusion in development of renal microcirculatory dysfunction in endotoxemic rats. *Intensive Care Med* 2011; **37**:1534–1542.

30 Boctor FN, Prichard JW. Kidney involvement in thrombotic thrombocytopenic purpura and malignant hypertension. *Transfusion* 2009; **49**:1783–1784.

31 Tsai HM. The kidney in thrombotic thrombocytopenic purpura. *Minerva Med* 2007; **98**:731–747.

32 Tsai HM. Shear stress and von Willebrand factor in health and disease. *Semin Thromb Hemost* 2003; **29**:479–488.

33 Abdulkader RC, Liborio AB, Malheiros DM. Histological features of acute tubular necrosis in native kidneys and long-term renal function. *Ren Fail* 2008; **30**:667–673.

34 Kiss N, Hamar P. Histopathological evaluation of contrast-induced acute kidney injury rodent models. *Biomed Res Int* 2016; **2016**:3763250.

35 Lambers M, Goldenberg NA, Kenet G, Kirkham FJ, Manner D, Bernard T, *et al.* Role of reduced ADAMTS13 in arterial ischemic stroke: a pediatric cohort study. *Ann Neurol* 2013; **73**:58–64.

36 Cao WJ, Niiya M, Zheng XW, Shang DZ, Zheng XL. Inflammatory cytokines inhibit ADAMTS13 synthesis in hepatic stellate cells and endothelial cells. *J Thromb Haemost* 2008; **6**:1233–1235.

37 Zheng XL. Structure-function and regulation of ADAMTS-13 protease. *J Thromb Haemost* 2013; **11 (Suppl 1)**:11–23.

38 Saitta B, Jalili MF, Zohoorkari H, Rao R, Hallows KR, Baty CJ, *et al.* Ex vivo kidney slice preparations as a model system to study signaling cascades in kidney epithelial cells. *Methods Cell Biol* 2019; **153**:185–203.

39 Marchi R, Rojas H. Effect of von Willebrand factor on clot structure and lysis. *Blood Coagul Fibrinolysis* 2015; **26**:533–536.

40 Wu Y, Liu W, Zhou Y, Hilton T, Zhao Z, Liu W, *et al.* von Willebrand factor enhances microvesicle-induced vascular leakage and coagulopathy in mice with traumatic brain injury. *Blood* 2018; **132**:1075–1084.

41 Peyvandi F, Garagiola I, Baronciani L. Role of von Willebrand factor in the haemostasis. *Blood Transfus* 2011; **9 Suppl 2**:s3–s8.

42 Coppo P, Lammle B. Animal models of thrombotic thrombocytopenic purpura: the tales from zebrafish. *Haematologica* 2020; **105**:861–863.

43 Vanhoorelbeke K, De Meyer SF. Animal models for thrombotic thrombocytopenic purpura. *J Thromb Haemost* 2013; **11 (Suppl 1)**:2–10.

44 Schiviz A, Wuersch K, Piskernik C, Dietrich B, Hoellriegl W, Rottensteiner H, *et al.* A new mouse model mimicking thrombotic thrombocytopenic purpura: correction of symptoms by recombinant human ADAMTS13. *Blood* 2012; **119**:6128–6135.

45 Wirtz MR, van den Brink DP, Roelofs J, Goslings JC, Juffermans NP. Therapeutic application of recombinant human ADAMTS-13 improves shock reversal and coagulation status in a trauma hemorrhage and transfusion rat model. *Intensive Care Med Exp* 2020; **8**:42.